Article

Electrochemiluminescent Graphene Quantum Dots as A Sensing Platform: A Novel Dual Amplification for MicroRNA Assay

Pu Zhang, Ying Zhuo, Yuanyuan Chang, Ruo Yuan, and Yaqin Chai

Anal. Chem., **Just Accepted Manuscript** • DOI: 10.1021/acs.analchem.5b02495 • Publication Date (Web): 28 Sep 2015

Electrochemiluminescent Graphene Quantum Dots as A Sensing Platform: A Novel Dual Amplification for MicroRNA Assay

Pu Zhang, Ying Zhuo, Yuanyuan Chang, Ruo Yuan*, Yaqin Chai*

Key Laboratory of Luminescent and Real-Time Analytical Chemistry (Southwest University), Ministry of Education, College of Chemistry and Chemical Engineering, Southwest University, Chongqing 400715, PR China

* Corresponding author. Tel.: +86-23-68252277; Fax: +86-23-68253172.

E-mail address: yuanruo@swu.edu.cn; yqchai@swu.edu.cn

ABSTRACT

Graphene quantum dots (GQDs) with an average diameter as small as 2.3 nm were synthesized to fabricate an electrochemiluminescence (ECL) biosensor based on T7 exonuclease-assisted cyclic amplification and three-dimensional (3D) DNA-mediatedsilver enhancement for microRNA (miRNA) analysis. Herein, to overcome the barrier in immobilizing GQDs, aminated-3,4,9,10-perylenetetracarboxylic acid (PTCA-NH_2) was introduced to load GQDs through π-π stacking (GQDs/PTCA-NH_2), realizing the solid-state GQDs application. Furthermore, Fe_3O_4-Au core-shell nanocomposites (Au@Fe_3O_4) was adopted as probe anchor to form a novel electrochemiluminescent (ECL) signal tag of GQDs/PTCA-NH_2/Au@Fe_3O_4. The prepared ECL signal tag was decorated on the electrode surface, exhibiting excellent film-forming performance, good electronic conductivity and favorable stability, all of which overcame the obstacle for applying GQDs in ECL biosensing and showed a satisfactory ECL response under the co-reactant of $S_2O_8^{2-}$. Afterwards, hairpin probe modified on the electrode was opened by helper DNA, followed by assembling target to hybridize with the exposed stem of helper DNA. Significantly, T7 exonuclease was employed to digest DNA/RNA duplex and trigger the target recycling without asking for a specific recognition site in the target sequence, realizing a series of RNA/DNA detection by changing the sequence of the complementary DNA. At last, ECL signal was further enhanced by AgNPs-based 3D DNA networks. After the two amplifications, the ECL signal of GQDs was extraordinarily increased and the prepared biosensor achieved a high

sensitivity with the detection limit of 0.83 fM. The biosensor was also explored in real samples and the result was in good accordance with the performance of qRT-PCR. Considering the excellent sensitivity and applicability, we believe that the proposed biosensor is a potential candidate for nucleic acid biosensing.

KEYWORDS: electrochemiluminescent, graphene quantum dots, microRNA, biosensor, T7 exonuclease, Ag nanoparticles enhancement.

INTRODUCTION

Graphene quantum dots (GQDs), one of the most fascinating graphene materials, amazed us on the horizon of new luminescent nanomaterial with extraordinary properties of low toxicity, excellent solubility, satisfactory surface grating and better biocompatibility[1]. The reported synthesis technique of GQDs can be divided into two categories: bottom-up[2-4] and top-down[5,6] method. The top-down strategy, which is mainly depended on cleaving along the oxygen-containing functional groups of graphene oxide (GO) and cutting down the large sheet of graphene into smaller sheets, has appealed more attention due to the merits of large scale production, plentiful raw materials and easy operation. For example, Zhu et al.[7] have reported a facile top-down microwave-assisted method for preparing electrochemiluminescent GQDs from GO nanosheets with acid treatment and the obtained GQDs performed excellent optical properties. Inspired by that, we attempt to leave out the additional apparatus (microwave irradiation) to synthesize GQDs in a more easy and inexpensive way.

The inherent virtues of GQDs drive the dreams of exploring its possible applications in electrochemiluminescence (ECL) which is superior to the traditional protocols due to the merits of low cost, easy operation and high detection sensitivity[8]. However, a central challenge in the practical application of GQDs is the prevention of water solubility, which is of great significance because most of the studies put the GQDs in aqueous solution or modify with a DNA strand for analysis in current time[8,9]. Therefore, to find a functional material to realize solid-state GQDs ECL is imminently needed. A promising approach to solve this problem is to find an ideal candidate to

immobilize GQDs. Aminated-3,4,9,10-perylenetetracarboxylic acid (PTCA-NH_2), with advantages of high specific surface area, outstanding film-forming performance and satisfying electronic property[10], served as substrate to realize the solid-state GQDs ECL detection through π-π stacking. Immobilizing GQDs on the surface of the electrode could decrease the usage of GQDs, shorten the distance of electronic transmission, improve the efficiency of the ECL response and ensure the stability of the sensor on account of the π-electron delocalization of PTCA-NH_2[11].

To achieve high detection sensitivity, another major effort is aimed at improving the ECL response of GQDs. It has been revealed that silver nanoparticles (AgNPs) could reduce the electron-relay shield between semiconducting ECL emitters and the working electrode due to the outstanding conductivity and fascinating biocompatibility, accelerating the electron-/hole-injecting rate[12,13], thus remarkably enhancing the ECL response. Enlightened by this property of AgNPs, we employed AgNPs to enhance the ECL emission of GQDs and obtained a satisfactory ECL response. In order to increase the amount of AgNPs, we deposited the AgNPs in the three-dimensionalm (3D) DNA skeleton owing to the high affinity between metal cations and DNA[14-16]for enhancing the ECL response of GQDs. Up to now, the existing researches by employing GQDs in ECL field were mainly focused on the detection of various cations[17,18] and proteins[19], while little attention has been received in microRNA (miRNA) detection field. In consideration of the significant roles of miRNAs in various biological analysis[20,21], it is promising to generalize the application of GQDs in ECL fields for miRNA analysis.

Recently, the new platform focused on improving the sensitivity of miRNA detection is highly desired. T7 exonuclease has been reported to degrade RNA and DNA from RNA/DNA hybrids in the 5′ to 3′ direction but is unable to degrade either double-stranded or single stranded RNA[22]. Significantly, T7 exonuclease-assisted cyclic enzymatic amplification method (CEAM) is developed for sensitive, rapid and price moderate detection of nucleic acids, which does not ask for a specific recognition site in the target sequence[23]. Taking advantage of this property, we try to realize a series of RNA/DNA detection by changing the corresponding sequences of the hybridized DNA. According to our knowledge, few attentions have been paid to the employment of T7 exonuclease-assisted CEAM to detect miRNA in ECL system.

As illustrated in Scheme 1, a GQDs-realized ECL biosensor based on T7 exonuclease-induced target recycling and 3D DNA-mediated silver enhancement was successfully constructed for miRNA detection. Initially, the GQDs were synthesized by refluxing GO with concentrated acid and assembled with PTCA-NH_2 through π-π stacking (GQDs/PTCA-NH_2).Afterwards, Fe_3O_4-Au core-shell nanocomposites (Au@Fe_3O_4) was employed onto the prepared composites through Au-N bond to anchor numerous DNA probes (GQDs/PTCA-NH_2/Au@Fe_3O_4), in which Au nanoparticles (AuNPs) could accelerate the electron transfer and the introduction of Fe_3O_4 realized the magnetic separation. Following that, the GQDs/PTCA-NH_2/Au@Fe_3O_4 was introduced onto the electrode surface for the capture of hairpin probe (HP) through Au-N bond. Subsequently, the helper DNA could further hybridize with target miRNA to open the hairpin structure of HP. With

the aid of T7 exonuclease, the hybridized DNA/RNA duplexes were digested and released miRNA to trigger another cycle. As outlined in Scheme 1, single stranded DNA H1, H2, H3 and crosslink 1, crosslink 2 were immobilized on the electrode through hybridizing with opened hairpin probe to self-assemble into a 3D Y-shaped nanostructure. Then Ag nanoparticles (AgNPs) were in situ reduced in the 3D DNA skeleton due to electrostatic interactions. The proposed dual amplification brought about an extremely high sensitivity under the co-reactant of $S_2O_8^{2-}$ with a detection limit of 0.83 fM for miRNA detection. It is worth pointing out that this biosensor not only realized the immobilization of GQDs on the electrode surface but also performed desirable detection limit and selectivity. Moreover, this method can be expanded to detect a series of RNA/DNA detection by changing the sequence of the complementary DNA.

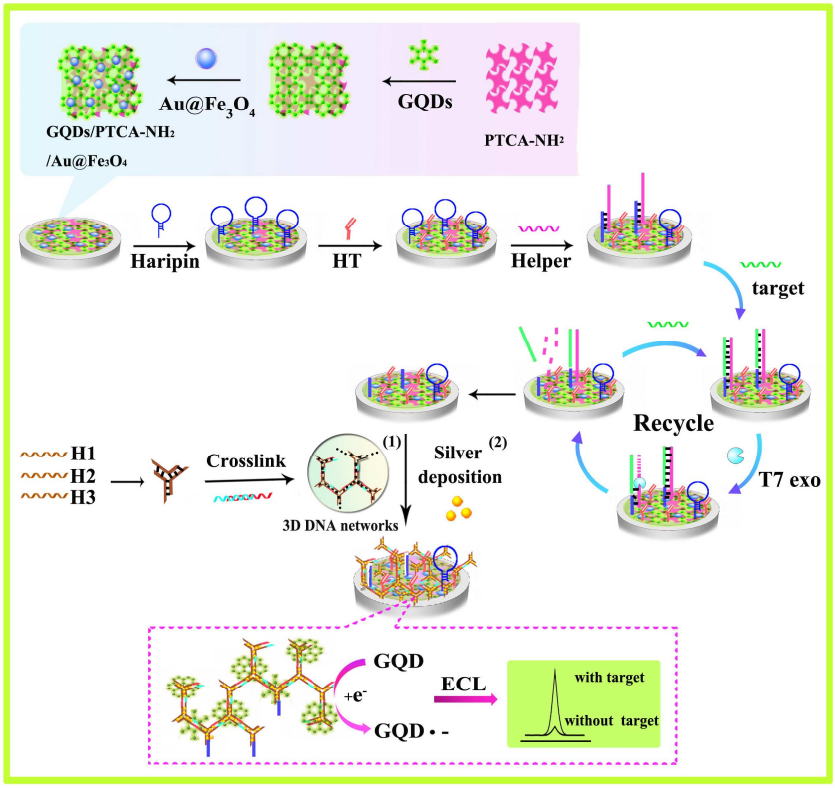

Scheme 1. Designed illustration of the proposed biosensor and ECL reaction mechanism for sensitive detection of miRNA.

EXPERIMENTAL METHODS

Chemical agents and devices Graphene oxide was purchased from Nanjing Xianfengnano Co. (Nanjing, China). Au@Fe_3O_4 (shell/core) magnetic beads (5 mg mL^{-1}, 50 nM in diameter) were obtained from Xi'an Gold Mag Nanobiotech Co. (Xi'an, China). PTCA was obtained from Lian Gang Dyestuff Chemical Industry Co. (Liaoning, China). Hydroquinone and $K_2S_2O_8$ was purchased from Shanghai chemical Reagent Co. (Shanghai, China). $AgNO_3$ was obtained from Kelong Chemical Company (Chengdu, China). Phosphate buffered solution (PBS) (pH 7.4, 0.10 M) were deployed with 0.1 M Na_2HPO_4, 0.1 M KH_2PO_4 and 0.1 M KCl. Ferricyanide solutions ($Fe(CN)_6^{3-/4-}$, 5mM, pH 7.4) were obtained by dissolving potassium

ferricyanide and potassium ferrocyanide with PBS buffer (pH 7.4). HT (96%) was purchased from Sigma-Aldrich Chemical Co. (USA). T7 exonuclease and 10×NEBuffer 4 were obtained from New England Biolabs (USA). The buffer to dilute the hybridizations was prepared by the mix of 10 mM Tris-HCl, 1 M NaCl, 1 mM EDTA, pH 7.0.

Oligonucleotides used in this work were custom-made by TaKaRa (Dalian, China) and the sequences of the oligonucleotides were as follows:

Hairpin Probe: 5'-NH_2-TCT TGG ACA CAG TAA AGA GAG GTG CGC CCA TTG TGT CCA AGA ACA ACT ATC AGA TCT-3'

Helper DNA: 3'-AGA ACC TGT GTC ATT TCT CTC CAC GCG GGT AAC ACA GGT TCT TGT TGA TAG TCT AGA AAT TAC GAT TAG CAC TAT CCC CA-5'

MiRNA-155: 5'-UUA AUG CUA AUC GUG AUA GGG GU-3'

H1: 5'-TGT TGA TAG TCT AGA ACA TGA AAA GAT TGG GAT ATA GTA TAA GGA T-3'

H2: 5'-TGT TGA TAG TCT AGA ATC CTT ATA CTA TAT CCC ACC TGA CTC CTG TGG AGA AG-3'

H3: 5'-TGT TGA TAG TCT AGA CTT CTC CAC ACC CCC CGG AGT CAG GTG CAA TCT TTT CAT GT-3'

Crosslink 1: 5'-TCT AGA CTA TCA ACA ACT AGA TAC ATA CAG-3'

Crosslink 2: 5'-TCT AGA CTA TCA ACA CTG TAT GTA TCT AGT-3'

MiRNA-101: 5'-UAC AGU ACU GUG AUA ACU GAA-3'

Single-base mismatch (sRNA):5'-UUAAGGCUAAUCGUGAUAGGGGU-3'

Cyclic voltammetry (CV) was performed with a CHI 660C electrochemical workstation (Shanghai Chenhua Instrument, China) by scanning the potential from 0.2 to 0.6 V at a scan rate of 0.05V s^{-1}. The ECL exploration was measured with a model MPI-A ECL analyzer (Xi'an Remax Electronic Science & Technology Co., Xi'an, China) with the voltage of 800 V and the potential was set from -1.6 to -0.4 V at a scan rate of 0.3 V s^{-1}. All experiments were proposed in a conventional three-electrode system: a platinum wire was the counter electrode, Ag/AgCl (sat. KCl) was the reference electrode and the modified glassy carbon electrode (GCE, Φ=4mm) was working electrode. High-resolution transmission electron microscope (HRTEM) images were achieved with a JEM 1200EX microscope (JEOL, Japan). Transmission electron micrograph (TEM) graphs were obtained with a Tecnai G2 F20 microscope (FEI Co. USA). Atomic force microscopy (AFM) detections were analyzed with dimension icon microscopy (Bruker Co. Ger.). X-ray photoelectron spectroscopy (XPS) analysis was carried out with a VG Scientific ESCALAB 250 spectrometer operating by Al Ka X-ray (1486.6 eV) as the light source. The fourier transform infrared spectroscopy (FTIR) was recorded on a Nexus 670 FTIR spectrophotometer using a KBr pellets (Nicolet Instruments).

Preparation of GQD nanomaterials GQDs were synthesized by GO solution (30 mL, 0.5 mg·mL^{-1}) which was mixed with concentrated H_2SO_4 (2 mL) and HNO_3 (8 mL). Then, the mixture was refluxed at 180 °C for 6 h. Then the product consisted of a brown transparent suspension was cooled to room temperature. The suspension

was centrifuged for several times and the pH was tuned to 8.0. Finally, the mixture was dialyzed in a dialysis bag (molecular weight cut off 10-14 kDa) to yield ECL GQDs.

Preparation of GQDs/PTCA-NH_2 1 g 3,4,9,10-perylenetetracarboxylic dianhydride (PTCDA) was dispersed in 5 mL acetone, then 20 mL ethanediamine was added and stirred at 4 ℃ for 2 h. Followed by centrifugation and rinsing with distilled water several times until the pH of the upper solution was 7.0, and the aminated PTCA (PTCA-NH_2)was obtained. Then PTCA-NH_2 was attached to GQDs through π-π interactions: 5 mL PTCA-NH_2 and 5 mL GQDs solution were mixed together and stirred at room temperature for 48 h to obtain the GQDs/PTCA-NH_2 hybrid nanocomposite.

Preparation of GQDs/PTCA-NH_2/Au@Fe_3O_4 The GQDs/PTCA-NH_2 nanocomposite was dispersed in 5 mL Au@Fe_3O_4 and stirred for 16 h. Owing to the strong interaction between the -NH_2 and Au, Au@Fe_3O_4 could attached on the GQDs/PTCA-NH_2 to achieve the GQDs/PTCA-NH_2/Au@Fe_3O_4 nanocomposite. The final product was collected and removed from the solution by employing an external magnetic field and then dispersed in 10mL double distilled water, stored at 4 ℃ for further use.

Fabrication of the proposed biosensor The schematic representation of the stepwise fabrication process for the prepared biosensor is shown in Scheme 1. Prior to surface modification, the GCE (Φ=4 mm) was polished with alumina slurry, followed by sonicating in anhydrous ethanol and double distilled water each for 5 min. The

cleaned GCE was firstly coated with 8 μL GQDs/PTCA-NH_2/Au@Fe_3O_4 solution. After drying in air, 10 μL of 2.5 μM HP was introduced on the surface of the electrode with 16 h incubation at room temperature, followed by immersing in 1 mM HT for 40 min. Then 10 μL helper DNA was dropped onto the electrode for 2 h. Then target RNA was introduced on the resulted electrode for 2 h at room temperature. Subsequently, the surface of electrode was incubated with 5 μL of 1×NEB buffer containing T7 exonuclease for 60 min. Afterwards, a droplet of a 25 μL mixture solution containing H1, H2, H3, Crosslink 1 and Crosslink 2 was casted onto the pretreated electrode for 2 h. 10 μL $AgNO_3$ (0.1 M in NH_4OH, pH 10.5) was dipped onto the prepared substrate for 15 min to absorb Ag^+ on the DNA skeleton. After washing with double distilled water, 10 μL hydroquinone was placed on the electrode to reduce the Ag^+ for 15 min. Finally, the AgNPs were grown in 10 μL of citrate buffer for 8 min. The ECL response of the designed biosensor was detected in the presence of 0.1 M $K_2S_2O_8$ as co-reactant.

RESULTS AND DISCUSSION

Characteristics of the nanomaterials Fig. 1A displayed a HRTEM graph of the GQDs. The diameters of the GQDs were distributed mainly over the range 1.7-3.3 nm with an average diameter of 2.3 nm and the size distributed homogeneously (as shown in Fig. 1B). In order to investigate the successful synthesis and the optical performance of the GQDs, UV-vis absorption was also explored (Fig S1 in the supporting information). The results were in good agreement with the previous study[7]. AFM images of GO and the GQDs were showed in Fig 2, the topographic heights of

GQDs were between 1nm and 1.5 nm (Fig 2CD), suggesting that the prepared GQDs were single layered or bilayered[24,25], comparing with the height of GO (Fig 2AB). To further study the ECL property of the prepared GQDs, ECL spectrum was observed by detecting the maximum ECL signal with a series of optical filters. As can be seen in Fig S3B, the ECL maximum emission wavelength of the GQDs was measured to be about 520 nm. Besides, we have made a comparison among the ECL emission spectroscopy of grapheme oxide (GO), GQDs/PTCA-NH_2/Au@Fe_3O_4 and modified with AgNPs (Fig S3-S4 in the supporting information). And the photoluminescence were carried out to further confirm the luminescent properties of GOQs (Fig S5 in the supporting information).

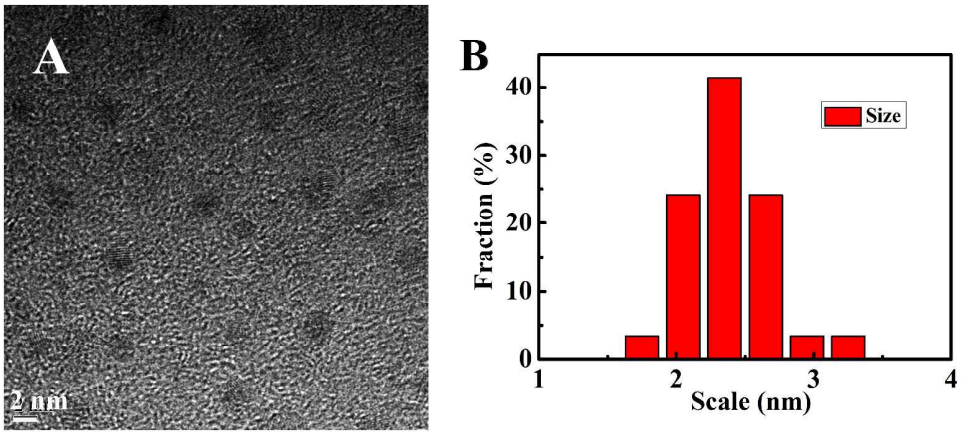

Fig 1. (A) HRTEM graph of synthesized GQDs. (B) Size distributions of GQDs.

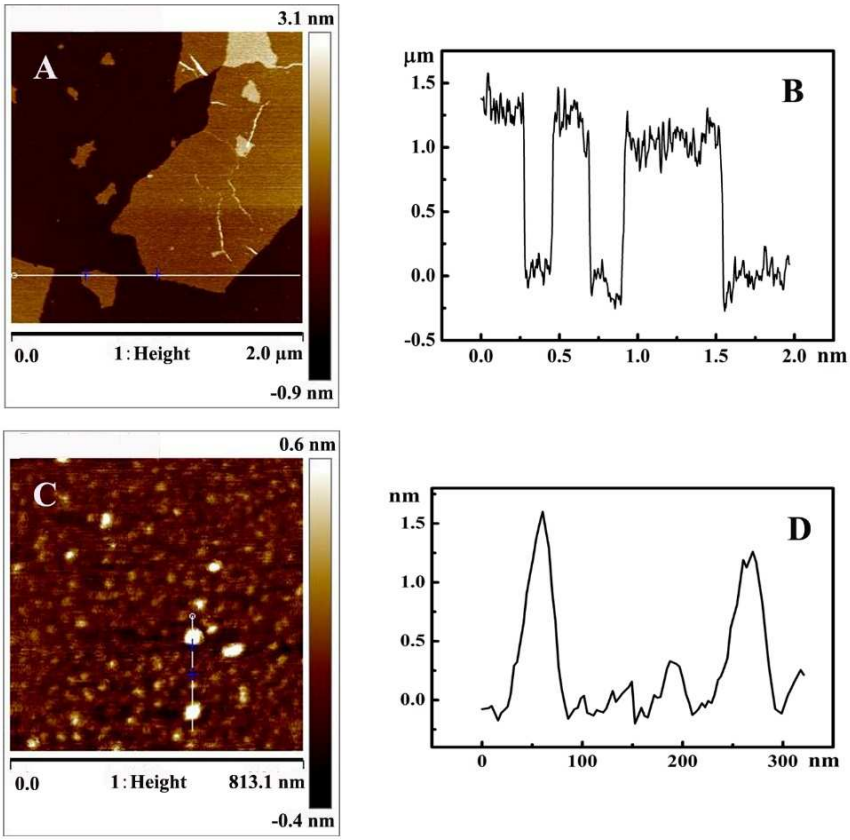

Fig 2. AFM graphs and their corresponding height profiles of GO (AB) and GQDs (CD).

The morphology of GQDs/PTCA-NH_2 and GQDs/PTCA-NH_2/Au@Fe_3O_4 were characterized by TEM. The self-assembly of GQDs on the surface of PTCA-NH_2 was proved by Fig. 3A, the as-synthesized PTCA-NH_2 nanomaterials performed irregular clavate-like structure and there can be found homogeneous and dense GQDs were covered on PTCA-NH_2. When Au@Fe_3O_4 was attached on GQDs/PTCA-NH_2 through Au-N bond, it was observed that Au@Fe_3O_4 with a diameter of 50 nm was stack on the surface of GQDs/PTCA-NH_2, suggesting the successful synthesis of GQDs/PTCA-NH_2/Au@Fe_3O_4 nanocomposites (Fig. 3B).

To further demonstrate the synthesis of GQDs/PTCA-NH_2/Au@Fe_3O_4, XPS was

studied for elemental analysis. As can be depicted in Fig. 4A, XPS analysis of Fe2p doublet (710.2 eV and 724.1 eV) was obtained, suggesting the existence of Fe element. As we can see in Fig. 4B-E, the spectra of O1s, N1s, C1s and Au4f can be observed, assigning to 531.2 eV and 533.4 eV, 400 eV, 285 eV, 83.3 eV and 87.0 eV, respectively. Under the elemental analysis, we could determine that the proposed GQDs/PTCA-NH_2/Au@Fe_3O_4 was successfully prepared. Besides, the typical FTIR spectroscopy was used to represent GQDs/PTCA-NH_2/Au@Fe_3O_4(Fig S2.in the supporting information).

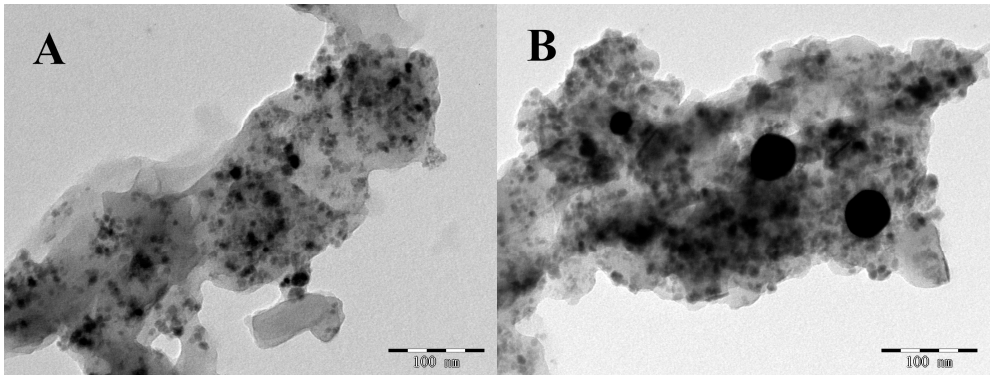

Fig 3. TEM images of (A) GQDs/PTCA-NH_2, (B) GQDs/PTCA-NH_2/Au@Fe_3O_4.

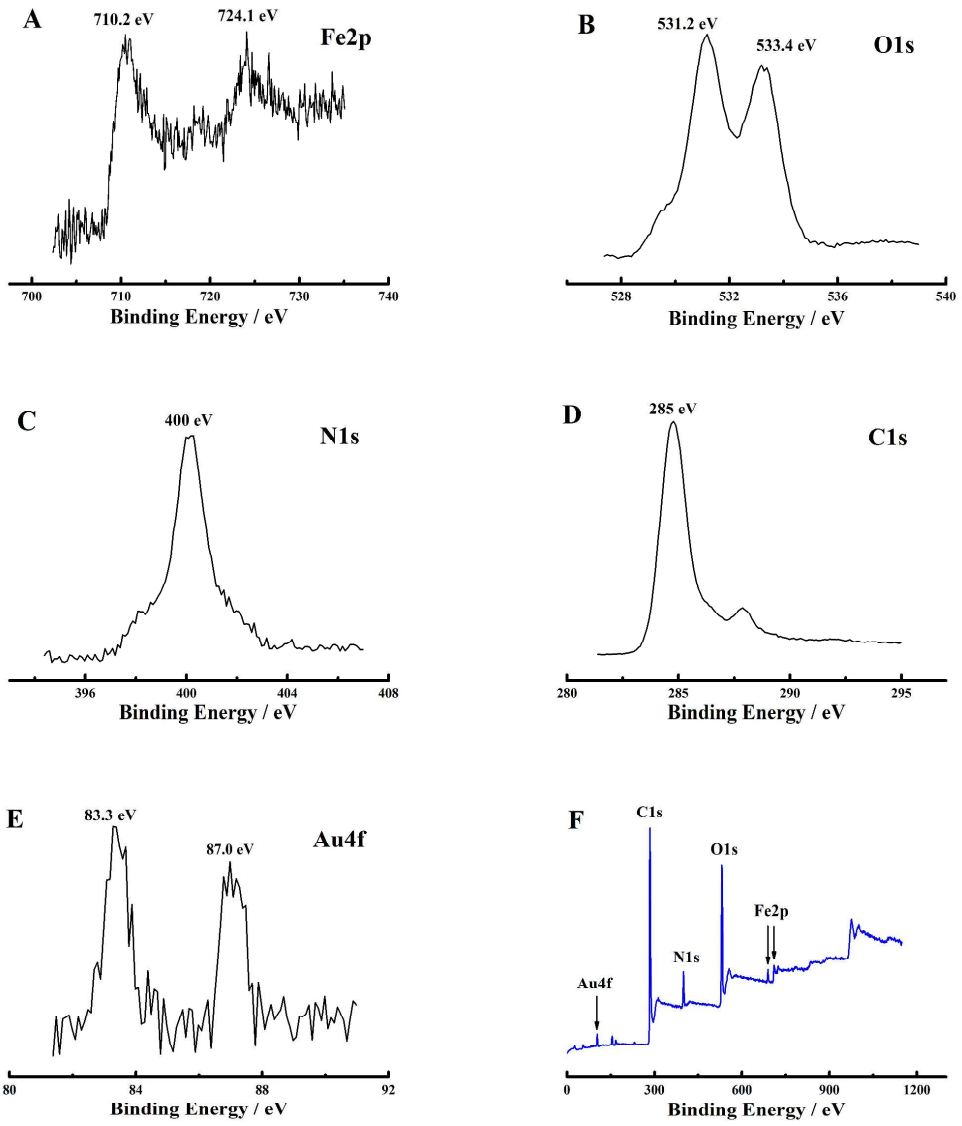

Fig 4. XPS analysis for GQDs/PTCA-NH_2/Au@Fe_3O_4.

The electrochemical performance of the biosensor The electrochemical characterization of the stepwise modified electrode was obtained by cyclic voltammetry (CV) and was showed in Fig. 5A. There was a couple of quasi-reversible redox peaks of the biosensor obtained in the bare electrode (curve a). When GQDs/PTCA-NH_2/Au@Fe_3O_4 was introduced onto the electrode, there was a remarkable increased current (curve b) because GQDs/PTCA-NH_2/Au@Fe_3O_4 was

used as an electro-conductive material for the acceleration of the electron transfer. After the adsorption of the hairpin probe, an obviously decreased peak current was achieved because of its feature of obstructing the electron transfer (curve c). Followed by employing HT to block nonspecific binding sites, a successively decline was detected (curve d). After helper DNA was successfully immobilized onto the electrode, we obtained a decreased current (curve e). The current further declined after incubating with target (curve f), which could be attributed to the hindrance of the electron transfer. As expected, the current responses were highly enhanced when the electrode was further treated with T7 exonuclease (curve g) which triggered the target recycling.

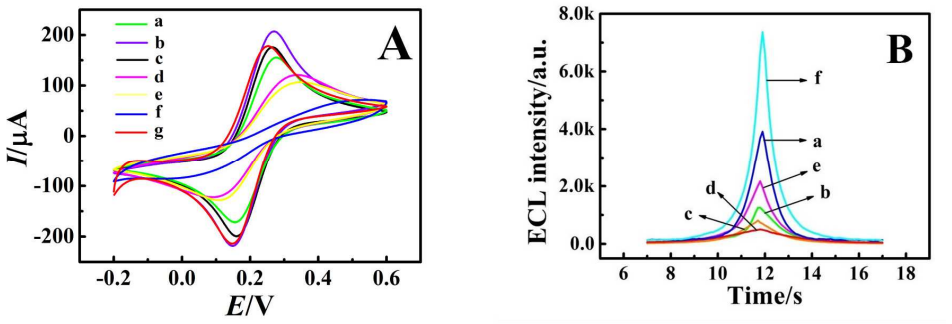

Fig 5. (A) CV profiles of proposed biosensor: bare GCE (curve a), decorated with PTCA-NH_2/Au@Fe_3O_4/GQDs (curve b), modified with hairpin probe (curve c), blocked with HT (curve d), introduced with helper DNA (curve e), employed with miRNA (curve f) and triggered by T7 exonuclease (curve g) in 5.0 mM $[Fe(CN)_6]^{3-/4-}$ at scan rate of 100 mV s^{-1}. (B) ECL-time curves of the proposed biosensor: incubation of GQDs/PTCA-NH_2/Au@Fe_3O_4 (curve a), immobilized with HP and HT (curve b), introduction of helper DNA (curve c), immobilization of miRNA (curve d), employment of T7 exonuclease (curve e) and modified with AgNPs (curve f);

potential v v window, -0.4 to 1.6 V; concentration of $K_2S_2O_8$, 0.1 M in PBS solution (pH=7.4).

The ECL performance of the biosensor The fabrication process of the biosensor was characterized in 0.1 M PBS (pH 7.4) containing 0.1 M $S_2O_8^{2-}$. The corresponding results are shown in Fig 5B. When PTCA-NH_2/Au@Fe_3O_4/GQDs was incubated on the electrode, an initial ECL intensity was acquired (curve a). When HP and HT (curve b) were successively introduced on the proposed electrode, the ECL signal declined accordingly. Then Helper DNA was coated on the electrode resulting to the decreased ECL signal (curve c). After the immobilization of the target RNA, noticeable decrease in ECL signal was observed (curve d). The ECL response was enhanced after employing with T7 exonuclease (curve e). Finally, the ECL signal was significantly raised (curve f), which was mainly attributed to that AgNPs intercalated into the DNA skeletons and could catalyze the ECL signal of GQDs. The employment of AgNPs was significant for the final enhancement of detection sensitivity.

The possible ECL mechanisms for the signal amplification strategy

As the previous studies, the possible mechanisms for the ECL response of GQDs in the presence of $S_2O_8^{2-}$ were described with the following equations:

$$GQDs + ne^- \rightarrow nGQDs^{\bullet -} \quad (1)$$

$$S_2O_8^{2-} + e^- \rightarrow S_2O_8^{\bullet 2-}$$

$$S_2O_8^{\bullet 2-} \rightarrow SO_4^{2-} + SO_4^{\bullet -}$$

$$GQDs^{\bullet -} + SO_4^{\bullet -} \rightarrow GQDs^* + SO_4^{2-}$$

$$GQDs^* \rightarrow GQDs + h\nu$$

In order to assess the possible effect of AgNPs in the ECL process, the CV responses of GQDs and GQDs modified with AgNPs were carried out (shown in Fig 6). It was observed that the onset of reduction potential of GQDs-AgNPs shifted positively and the reduction peak was increased obviously compared with GQDs. The results suggested that the electron transfer from GQDs to Ag may reduce the electron density of GQDs, promoting the reduction of GQDs. And AgNPs reduced the potential obstruction of equation (1). Therefore, it was concluded that the participation of AgNPs improved the quantity of reduced GQDs ($GQDs^{\bullet -}$) and excited GQDs (GQDs*), enhancing the ECL response of GQDs significantly.

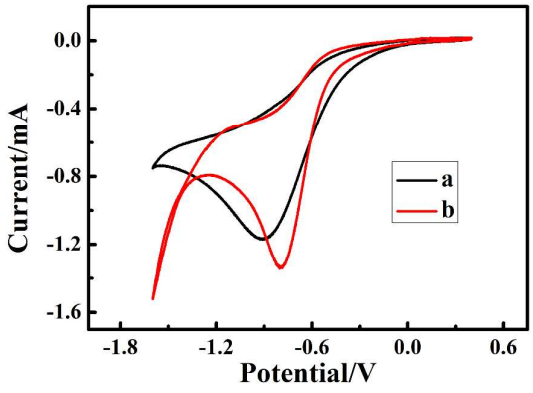

Fig 6. The CV responses of GQDs (a) and GQDs modified with AgNPs (b) in 0.1M PBS (pH 7.0) containing 0.1 M $S_2O_8^{2-}$.

ECL intensity of the proposed biosensor Under the optimized experimental conditions (Fig S6 in the supporting information), the sensitivity and the quantitative range of the miRNA biosensor were assessed by incubating with different concentrations of miRNA. The relationship between ECL response and concentrations of miRNA-155 was showed in Fig. 7. ECL signal increased gradually with the increasing concentration of miRNA. A linear relationship of ECL intensity and the

concentrations of miRNA was achieved in the range from 2.5 fM to 50 pM with the detection limit of 0.83 fM. The linear relationship could be represented as I = 9255.3 + 2617.8lg$c$, with the correlation coefficient of R^2= 0.996, where I is the ECL intensity and c is the concentration of miRNA-155. The ultrahigh sensitivity should be attributed to the high efficiency of the digestion of T7 exonuclease and the triple amplification strategy, which remarkably increased the ECL intensity.

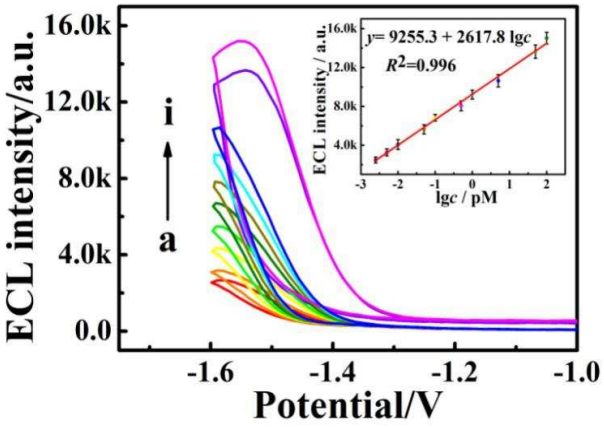

Fig 7. ECL-potential curves of the biosensor with the target concentration of (a) 2.5 fM, (b) 5 fM, (c) 0.01 pM, (d) 0.05 pM, (e) 0.1 pM, (f) 0.5 pM, (g) 1 pM, (h) 5 pM, (i) 50 pMin PBS solution (pH=7.4) containing 0.1 M $K_2S_2O_8$.

Stability, selectivity and reproducibility of the proposed biosensor The ECL stability of the proposed biosensor was detected using continuous cyclic scans for 23 cycles when optimizing the incubation time of T7 exonuclease. As can be seen in Fig. 8A, the ECL response did not show any significant changes. The experimental result indicated that the proposed biosensor had good stability.

As depicted in Fig. 8B, the selective recognition to miRNA of the biosensor was explored by investigating 500 pM of thrombin aptamer (TBA), 500 pM of PDGF

binding aptamer (PBA), 500 pM of sRNA and500 pM of miRNA-101, and to replace 50 pM of miRNA-155. The biosensor showed negligible cross-reactivity to TBA, PBA, sRNA,miRNA-101, and the mixture in the presence of miRNA-155 (50 pM) with interference substances despite their high concentrations, suggesting that only the perfectly matched sequence could trigger dual signal amplification strategies and the designed protocol had good selectivity toward target against other control sequences.

The reproducibility of the biosensor was explored by analysis of the same concentration of miRNA using five electrodes prepared in the same conditions and a relative standard deviation (RSD) of less than 5% was achieved, demonstrating that the reproducibility of the ECL biosensor was acceptable.

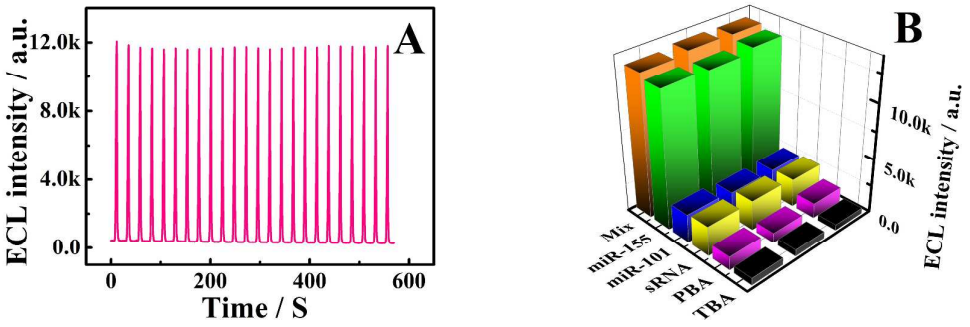

Fig 8. (A) ECL stability of the biosensor when detected for 23 cycles over 580 s. (B) Selectivity of the biosensor when analyzed with 500 pM of TBA, 500 pM of PBA, 500 pM of sRNA, 500 pM of miRNA-101, 50 pM of miRNA-155 and 50 pM of miRNA-155 in mixed solution.

Analytical application The practical applicability of the designed biosensor was studied by detecting miRNA-155 in biological cell lysates: Hela (cervical cancer cell line), HK-2 (human renal cubularepithelial cell line), L02 (normal hepatocyte cell line)

and22Rv1 (prostate carcinoma cell line). (The cell culture and total RNA extraction was showed in the supporting information). From results in Fig. 9, the proposed biosensor modified with cell lysate from Hela overexpressed in comparison with the blank buffer. When the biosensor was incubated with L02, the ECL response exhibited a low expression which was in accordance with the traditional qRT-PCR method. The obtained results were with consistence to qRT-PCR, which indicated that the prepared biosensor had potentiality in examination of miRNA-155 in real biological samples.

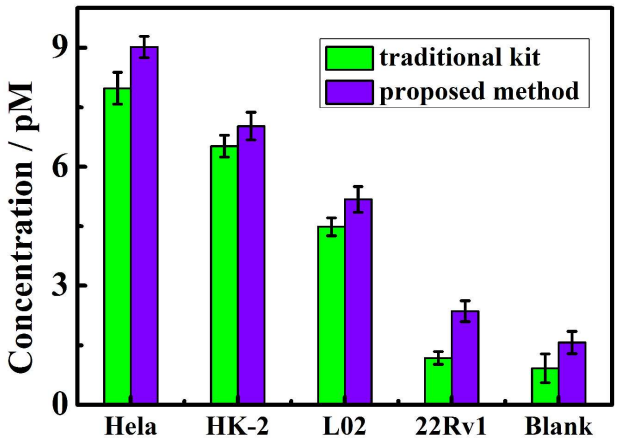

Fig 9. MiRNA-155 detection from different cell lysates.

CONCLUSIONS

A kind of homogeneous GQDs have been synthesized by refluxing GO with concentrated acid, which could produce high cathodic ECL emission under the assistance of dual amplification. The proposed ECL biosensor brings forth two innovative points. First of all, the modified nanomaterial (GQDs/PTCA-NH_2/Au@Fe_3O_4) was able to immobilize on the surface of the electrode with excellent film-forming property, ensuring the stability of the biosensor

and overcoming the good water-solubility of GQDs. Significantly, the ECL signal of GQDs could be improved by immobilizing GQDs on the electrode due to the smaller distance between luminescence reagent and the electrode surface. Secondly, the dual amplification devoted the biosensor to wide linear range and satisfying sensitivity. The T7 exonuclease-assisted cyclic amplification was introduced for the first amplified stage without demanding for a specific recognition site in the target sequence, realizing a series of RNA/DNA detection by changing the sequence of the complementary DNA. AgNPs-based 3D DNA networks were the second stage to enhance GQDs ECL signal and was significant for the final enhancement of detection sensitivity. Furthermore, our methods have challenged in the real samples and achieved satisfactory output. Relied on the instinctive properties proposed above, we anticipate that this sensing strategy can be expanded to explore an extensive range of DNA/RNA targets with reasonable design and hold significant potential bioanalysis.

ASSOCIATED CONTENT

Supporting Information

Additional electronic information as described in the essay is available free of charge via the Internet athttp://pubs.acs.org.

AUTHOR INFORMATION

*** Corresponding authors**

Tel.: +86 23 68252277, fax: +86 23 68253172.

E-mail addresses: yuanruo@swu.edu.cn (R. Yuan), yqchai@swu.edu.cn (Y. Q. Chai).

Notes

The authors declare no competing financial interest.

ACKNOWLEDGMENT

This work was financially supported by the NNSF of China (21575116, 51473136) and the Fundamental Research Funds for the Central Universities (XDJK2014C138).

REFERENCES

(1) Wang, L. L.; Zheng, J.; Li, Y. H.; Yang, S.; Liu, C. H.; Xiao, Y.; Li, J. S.; Cao, Z.; Yang, R. H. *Anal. Chem.***2014**, *86*, 12348−12354.

(2)Yan, X.; Li, Q. Q.; L, L. S. *J. Am. Chem. Soc.***2012**, *134*, 16095-16098.

(3) S, B. M.; Ángela, I. L. L.; Miguel, V. *Anal. Chem.* **2014***, 86,* 12279-12284.

(4) Yan, X.; Cui, X.; Li, B. S.; Li, L. S. *Nano Lett.* **2010**, *10*, 1869-1873.

(5) Li, Y.; Hu, Y.; Zhao, Y.; Shi, G.; Deng, L.; Hou, Y.; Qu, L. *Adv. Mater.***2011**, *23*, 776-780.

(6) D.Y.Pan , J.C. Zhang, Z. Li , M. H. Wu , Adv. Mater. 2010, 22,734-738.

(7)Li, L. L.; Ji, J.; Fei, R.; Wang, C. Z.; Lu, Q.; Zhang, J. R.; Jiang, L. P.; Zhu, J. J. *Adv. Funct. Mater.***2012**, *22*, 2971-2979.

(8)Dong, Y. Q.; Tian, W. R.; Ren, S. Y.; Dai, R. P.; Chi, Y. W.; Chen, G. N. *ACS Appl. Mater. Interfaces*. **2014**, *6*, 1646−1651.

(9) Lu, J. J.; Yan, M.; Ge, L.; Ge, S. G.; Wang, S. W.; Yan, J. X.; Yu, J. H. *Biosensors and Bioelectronics,* **2013***, 47*, 271–277.

(10) Chen, A. Y.; Gui, G. F.; Zhuo, Y.; Chai, Y. Q.; Xiang, Y.; Yuan, R. *Anal. Chem.* **2015***,87*, 6328-6334.

(11) Wang, X. Y.; Yun, W.; Dong, P.; Zhou, J. M.; He, P. G.; Fang, Y. Z. *Langmuir,***2008**, *24*, 2200-2205.

(12) Li, J. X.; Yang, L. X.; Luo, S. L.; Chen, B. B.; Li, J.; Lin, H. L.; Cai, Q. Y.; Yao, S. Z. *Anal. Chem.***2010**, *82*, 7357–7361.

(13) Deng, S. Y.; Ju, H. X. *Analyst*, **2013**, *138*, 43–61.

(14) Deng,Li.;Li,Yan.;Yan,X.P.;Xiao,J.;Ma,C.;Zheng,J.;Liu,S. J.;Yang, R. H. *Anal. Chem.***2015**, *87*, 2452−2458.

(15) Li, C. X.; Wang, H. Y.; Shen, J.; Tang, B. *Anal. Chem.***2015**, *87*, 4283−4291.

(16)Park, K. S.; Oh, S. S.; Sohbc, H. T.; Park, H. G. *Nanoscale*, 2014, **6**, 9977-9982.

(17) Zhang, Y.; Zeng, G. M.; Tang, L.; Chen, J.; Zhu, Y.; He, X. X.;He, Yan. *Anal. Chem.***2015**, *87*, 989−996.

(18) Li, L. L.; Wu, G. H.; Hong, T.; Yin, Z. Y.; Sun, D.; Abdel-Halim, E. S.; Zhu, J. J. *ACS Appl. Mater. Interfaces,***2014**, *6*, 2858−2864.

(19) Wang, Y.; Zhang, L.; Liang, R. P.; Bai, J. M.; Qiu, J. D. *Anal. Chem.***2013**, *85*, 9148−9155.

(20)Zhang, P.; Wu, X. Y.; Yuan, R.; Chai, Y. Q. *Anal. Chem.***2015**, *87*, 3202−3207.

(21) Qiu,X. P.;Liu,X.;Zhang,Wei.;Zhang,H.;Jiang,T. L.;Fan,D. L.; Luo, Y. *Anal. Chem.***2015**, *87*, 6303−6310.

(22) Wang,M.;Fu,Z. L.;Li,B. C.;Zhou,Y. L.;Yin,H. S.; Ai, S. Y. *Anal. Chem.***2014**, *86*, 5606−5610.

(23) Shinozaki, K.; Okazaki, T.; *Nucleic Acids Res.*, **1978**, *5*, 4245-4261.

(24) Zhou, X.; Zhang, Y.; Wang, C.; Wu, X.; Yang, Y.; Zheng, B.; Wu, H.; Guo, S.; Zhang, J.; *ACS Nano*, **2012**, *6*, 6592–6599.

(25) Ponomarenko, L. A.; Schedin, F.; Katsnelson, M. I.; Yang, R.; Hill, E. W.; Novoselov, K. S.; Geim, A. K. *Science*, **2008**,*320*, 356–358.

For TOC Only

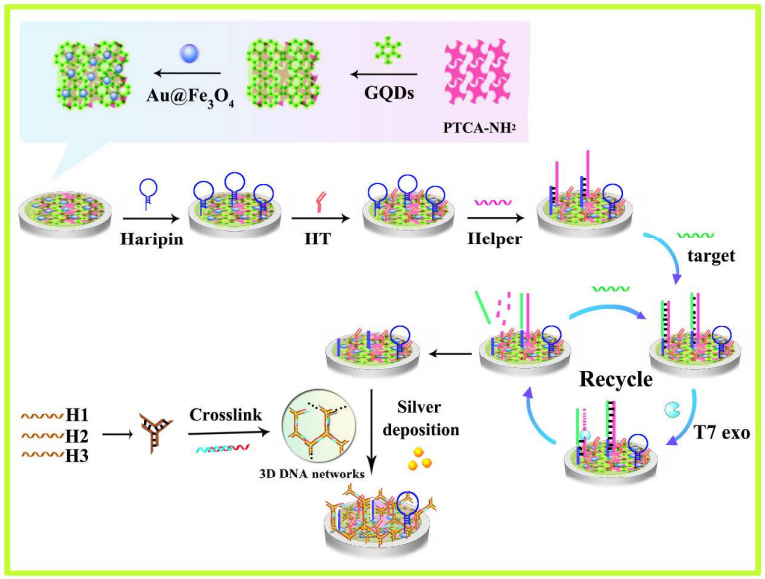
Au@Fe3O4
GQDs
PTCA-NH2
Haripin
HT
IIelper
target
Recycle
T7 exo
H1
H2
H3
Crosslink
3D DNA networks
Silver deposition